











Progress on lattice study of the chimera baryon spectrum in $Sp(4)$ gauge theory

C.-J. David Lin ,^{a,b,*} Ed Bennett ,^c Niccolò Forzano ,^d Deog Ki Hong ,^{e,f}
Ho Hsiao ,^{a,g} Jong-Wan Lee ,^h Biagio Lucini ,^{c,i} Maurizio Piai ,^d
Davide Vadacchino  and Fabian Zierler ^d

^a*Institute of Physics, National Yang Ming Chiao Tung University, Hsinchu 30010, Taiwan*

^b*Centre for High Energy Physics, Chung Yuan Christian University, Taoyuan 32023, Taiwan*

^c*Swansea Academy of Advanced Computing, Swansea University, Bay Campus, Swansea, SA1 8EN, UK*

^d*Department of Physics, Faculty of Science and Engineering, Swansea University, Singleton Park, Swansea, SA2 8PP, UK*

^e*Department of Physics, Pusan National University, Busan 46241, Korea*

^f*Extreme Physics Institute, Pusan National University, Busan 46241, Korea*

^g*Center for Computational Sciences, University of Tsukuba, Tsukuba, Ibaraki 305-8577, Japan*

^h*Particle Theory and Cosmology Group, Center for Theoretical Physics of the Universe, Institute for Basic Science, Daejeon, 34126, Korea*

ⁱ*Department of Mathematics, Faculty of Science and Engineering, Swansea University, Bay Campus, Swansea, SA1 8EN, UK*

^j*Centre for Mathematical Sciences, University of Plymouth, Plymouth, PL4 8AA, UK*

E-mail: dlin@nycu.edu.tw

Investigation of composite Higgs models (CHMs) is of importance in contemporary particle physics. In this article, we present lattice computations of the chimera baryon masses in $Sp(4)$ gauge theory with two and three Dirac flavours of hyperquarks (beyond the Standard Model fermions coupled to the $Sp(4)$ gauge fields) in the fundamental and antisymmetric representations, respectively. The chimera baryons are crucial for generating the Standard Model fermion masses through the partial compositeness mechanism in this gauge theory that can serve as the ultraviolet completion of the CHM with pseudo-Nambu-Goldstone bosons in the coset $SU(4)/Sp(4)$. Results shown here are primarily from a completed quenched computation, while those from our ongoing work with dynamical simulations are also discussed.

*The XVIth Quark Confinement and the Hadron Spectrum Conference (QCHSC24)
19-24 August, 2024
Cairns Convention Centre, Cairns, Queensland, Australia*

*Speaker

1. Introduction

The Standard Model (SM) of particle physics has been a success in explaining all the relevant experimental results hitherto. There are, nevertheless, motivations to search for physics beyond it. For instance, there is evidence that the Higgs-Yukawa sector of the SM suffers from the triviality problem that renders the cut-off scale indispensable (see, e.g., Refs. [1–7]), resulting in the unavoidable conclusion that the SM is an effective theory, and its ultraviolet (UV) completion has to be understood. It is also phenomenologically incomplete, as it cannot explain the observed baryon asymmetry of the universe [8, 9], nor the origin of its dark matter and dark energy components.

Despite the above compelling reasons to regard the SM as incomplete, neither direct nor indirect searches at the energy and precision frontiers have found any unambiguous evidence for physics beyond it. This means that the scale for new physics to emerge can be well above a few TeV. Therefore, any viable model that serves as a replacement of the SM Higgs-Yukawa sector must contain a scalar state (the Higgs boson) that is much lighter than new particles arising beyond the SM (BSM). This requirement makes it popular to design BSM models by resorting to quantum field theories containing pseudo-Nambu-Goldstone bosons (PNGBs). In this context, composite Higgs models (CHMs) have been attracting attention in the high energy physics community [10, 11]. These CHMs can be constructed with strongly interacting gauge theories that involve confinement and spontaneous breaking of approximate, global symmetry, which leads to the existence of naturally light bound-state Goldstone bosons. Amongst these confining theories [12], the $Sp(4)$ gauge theory with two Dirac flavours of hyperquarks (BSM fermions coupled to the $Sp(4)$ gauge fields) in the fundamental representation is particularly interesting [13, 14]. Due to the pseudo-reality of this gauge-group representation, in this model the global symmetry is $SU(4)$, spontaneously broken to $Sp(4)$ in the limit where hyperquarks are massless [15]. The coset, $SU(4)/Sp(4)$, then gives five PNGBs, with four of them interpreted as the degrees of freedom in the SM Higgs doublet. This is the minimal model that allows for the extension to address the issue of SM fermion masses, which we describe in the next paragraph.

In CHMs, the hierarchy between SM fermion masses can be explained through the mechanism of partial compositeness [16]. In this article, we use the top-quark mass for illustration. The implementation of the top partial compositeness is achieved in a CHM by first identifying in the spectrum of the new, strongly coupled theory a spin-1/2 bound state that carries the same quantum numbers as the top quark. This bound state, one of the chimera baryons described in this document, can then mix with the top quark and generate the mass of the latter. To realise this mechanism in the $Sp(4)$ gauge theory, it is convenient to introduce three Dirac flavours of hyperquarks in the two-index antisymmetric representation [13]. Since this representation is real, the global symmetry breaking pattern in this sector is $SU(6)/SO(6)$ [15]. The QCD $SU(3)$ gauge group is then embedded in the unbroken $SO(6)$, resulting in the fact that the antisymmetric hyperquarks are QCD-colour charged. Bound states composed of one antisymmetric and two fundamental valence hyperquarks, the chimera baryons, have the right quantum numbers to be identified as top partners.

Our collaboration started the research programme of *Theoretical Explorations on the Lattice with Orthogonal and Symplectic groups* (TELOS), in which we employ the tool of lattice field theory to examine various gauge theories that are interesting to the high-energy physics community. Investigation of the aforementioned $Sp(4)$ gauge theory with hyperquarks in two different represen-

Table 1: Lattice parameters and characterisation of quenched ensembles in this work, with β being the bare inverse lattice coupling constant, N_t and N_s being the number of temporal and spatial lattice sites, respectively. Here we also give the plaquette value, $\langle P \rangle$, and the gradient-flow scale w_0/a [49] (determined in our previous work in Ref. [30]), for all the ensembles.

Ensemble name	β	$N_t \times N_s^3$	$\langle P \rangle$	w_0/a
QB1	7.62	48×24^3	0.6018898(94)	1.448(3)
QB2	7.7	60×48^3	0.6088000(35)	1.6070(19)
QB3	7.85	60×48^3	0.6203809(28)	1.944(3)
QB4	8.0	60×48^3	0.6307425(27)	2.3149(12)
QB5	8.2	60×48^3	0.6432302(25)	2.8812(21)

tations has been the focus of our work¹. In the past few years, we have published several papers in this research direction [28–42], exploring measurable quantities such as the mass spectrum, decay constants, topology, and spectral densities². This article summarises the progress of our work on the spectrum of the chimera baryons. Most of the results presented here are obtained in calculations performed in the quenched approximation, as published in Ref. [38] with the data release in Ref. [47], while some exploratory results from our dynamical computations [48] are also reported.

2. Lattice implementation and ensemble parameters

In this work, lattice computations for $Sp(4)$ gauge theory are carried out using the Wilson plaquette action for the pure gauge sector. Hyperquarks are described by Wilson fermions. Details of the notation can be found in Sect. II.A of Ref. [38]. As mentioned in the previous section, we report mainly results from quenched calculations, where the fermion determinant is set to be a constant. Lattice parameters for the quenched ensembles used in this work are summarised in Tab. 1. We also report exploratory results from our fully dynamical simulations, obtained using the ensemble M2 with details given in Tab. 1 of Ref. [41].

We investigate the chimera baryon states sourced by the following operators (where Q and Ψ are the fundamental and antisymmetric hyperquark fields, respectively)

$$O_\rho^{ijk,5} \equiv Q_\alpha^{ia} (C\gamma^5)_{\alpha\beta} Q_\beta^{jb} \Omega^{ad} \Omega^{bc} \Psi_\rho^{kcd}, \quad (1)$$

$$O_\rho^{ijk,\mu} \equiv Q_\alpha^{ia} (C\gamma^\mu)_{\alpha\beta} Q_\beta^{jb} \Omega^{ad} \Omega^{bc} \Psi_\rho^{kcd}, \quad (2)$$

with α, β, ρ being spinor indices, i, j, k indicating the flavour quantum number, and a, b, c, d being hypercolour indices. In the above expressions, γ^5 and γ^μ are Dirac matrices, with C being the

¹Lattice studies for CHMs have also been performed by other collaborations for the gauge groups of $SU(2)$ [17–19] and $SU(4)$ [20–27].

²The $Sp(4)$ gauge theory has also been studied in the context of research in dark matter [43–46].

Table 2: Properties of the three lowest-lying flavoured chimera baryon states sourced by the interpolating operators in Eqs. (1) and (2) with flavour indices omitted. In addition to the spin quantum number, here we also list the representations of the unbroken global symmetry groups, $Sp(4)$ and $SO(6)$.

Chimera baryon	Interpolator	J	$Sp(4)$ repn	$SO(6)$ repn	QCD analogy
Λ_{CB}	O_{ρ}^5	1/2	5	6	Λ (1116)
Σ_{CB}	O_{ρ}^{μ}	1/2	10	6	Σ (1193)
Σ_{CB}^*	O_{ρ}^{μ}	3/2	10	6	Σ^* (1379)

matrix for the operation of charge conjugation. Furthermore, Ω is the symplectic matrix,

$$\Omega \equiv \begin{pmatrix} 0 & 0 & 1 & 0 \\ 0 & 0 & 0 & 1 \\ -1 & 0 & 0 & 0 \\ 0 & -1 & 0 & 0 \end{pmatrix}, \quad (3)$$

in the hypercolour space. The operator in Eq. (1) sources spin-1/2 states. On the other hand, $O_{\rho}^{ijk,\mu}$ in Eq. (2) overlaps with both spin-1/2 and 3/2 states, which can be distinguished using the projectors,

$$P_{1/2}^{\mu\nu} = \frac{1}{3}\gamma^{\mu}\gamma^{\nu}, \quad P_{3/2}^{\mu\nu} = \delta^{\mu\nu} - \frac{1}{3}\gamma^{\mu}\gamma^{\nu}. \quad (4)$$

Drawing analogy with QCD baryonic states, the three lowest-lying states sourced by the interpolators in Eqs. (1) and (2) are called Λ_{CB} , Σ_{CB} and Σ_{CB}^* . Their properties are summarised in Tab. 2. Amongst these three chimera baryons, Λ_{CB} and Σ_{CB} are candidates of the top partner [50]. Note that in this article we discuss only flavour off-diagonal chimera baryon states, and will not write the flavour indices explicitly below. We then compute the correlators for extracting masses of the above-mentioned chimera baryons. For Λ_{CB} , it is

$$C_{\Lambda_{\text{CB}}}(t) = \sum_{\vec{x}} \langle O_{\rho}^5(x) \overline{O_{\sigma}^5}(0) \rangle. \quad (5)$$

As for Σ_{CB} and Σ_{CB}^* , we have

$$C_{\Sigma_{\text{CB}}}(t) = P_{1/2}^{\mu\nu} C^{\mu\nu}(t), \quad C_{\Sigma_{\text{CB}}^*}(t) = P_{3/2}^{\mu\nu} C^{\mu\nu}(t), \quad (6)$$

with

$$C^{\mu\nu}(t) = \sum_{\vec{x}} \langle O_{\rho}^{\mu}(x) \overline{O_{\sigma}^{\nu}}(0) \rangle. \quad (7)$$

Note that we do not write explicitly the dependence on the spinor indices, ρ and σ , in $C_{\Lambda_{\text{CB}}}(t)$, $C_{\Sigma_{\text{CB}}}(t)$, $C_{\Sigma_{\text{CB}}^*}(t)$, and $C^{\mu\nu}(t)$. In the following, we will use the symbol, $C_{\text{CB}}(t)$, to denote a generic chimera-baryon correlator in Eqs. (5) and (6).

It should be noted that the interpolating operators in Eqs. (1) and (2) source both even and odd parity states. In fact, without an actual lattice numerical calculation, it is not easy to confirm the parity of the lowest-lying states appearing in the correlators in Eqs. (5) and (6). In other words, it requires a lattice calculation to determine the parity of Λ_{CB} , Σ_{CB} and Σ_{CB}^* . This will be discussed in the next section.

3. Analysis and numerical results

Since the interpolators in Eqs. (1) and (2) source both parity-even and -odd states, at large Euclidean time, a chimera-baryon correlator is expected to exhibit the behaviour,

$$C_{\text{CB}}(t) \xrightarrow{0 \ll t \ll T} P_+ \left[c_+ e^{-m^+ t} - c_- e^{-m^- (T-t)} \right] + P_- \left[c_- e^{-m^- t} - c_+ e^{-m^+ (T-t)} \right], \quad (8)$$

with T being the temporal lattice extent, and P_{\pm} being the parity projectors,

$$P_{\pm} = \frac{1 \pm \gamma_0}{2}. \quad (9)$$

The quantities m^{\pm} and c_{\pm} are masses and the baryon-to-vacuum transition amplitudes of the corresponding parity states. To proceed, we compute the ‘‘parity-projected’’ correlator,

$$\overline{C}_{\text{CB}}^{\pm}(t) = \frac{P_{\pm} C_{\text{CB}}(t) - P_{\mp} C_{\text{CB}}(T-t)}{2}. \quad (10)$$

It can be easily shown that the large-Euclidean-time behaviour of $\overline{C}_{\text{CB}}^{\pm}(t)$ is

$$\overline{C}_{\text{CB}}^{\pm}(t) \longrightarrow c_{\pm} e^{-m^{\pm} t} - c_{\mp} e^{-m^{\mp} (T-t)}. \quad (11)$$

Working in the regime $0 \leq t < T/2$, one can define the effective masses (in lattice units) for the parity-even and -odd states,

$$am_{\text{eff,CB}}^{\pm}(t) = \ln \left[\frac{\overline{C}_{\text{CB}}^{\pm}(t)}{\overline{C}_{\text{CB}}^{\pm}(t+1)} \right]. \quad (12)$$

Similarly, one can also calculate the effective mass using the unprojected correlator in Eq. (8),

$$am_{\text{eff,CB}}(t) = \ln \left[\frac{C_{\text{CB}}(t)}{C_{\text{CB}}(t+1)} \right]. \quad (13)$$

Upon examination of the effective masses in Eq. (12), one can determine the parity of the ground-state chimera baryons. Furthermore, the asymptotic behaviour of the effective mass computed through the unprojected correlator can serve as a crosscheck. One example is illustrated in Fig. 1, where we display these effective masses for states sourced by \mathcal{O}_{ρ}^5 . It is clear that the lightest chimera baryon in this channel (Λ_{CB}) is of even parity. We find the same conclusion for Σ_{CB} and Σ_{CB}^* .

In this work, we extract the chimera baryon masses, m_{CB} , from correlators at various fundamental and antisymmetric bare hyperquark masses, $m^{(f)}$ and $m^{(as)}$, on the ensembles listed in Tab 1. Using formulae inspired by heavy baryon chiral perturbation theory (HBChPT) [51, 52], with the inclusion of symmetry-breaking effects from lattice artefacts to $\mathcal{O}(a)$ [53], this enables us to investigate the hyperquark-mass dependence of m_{CB} . It also allows for the extrapolation to the continuum limit. We work at the order of the square of the hyperquark masses, *i.e.*, the fourth power of the fundamental and antisymmetric pseudoscalar-meson masses, m_{PS} and m_{ps} . As explained in detail in Ref. [38], it is challenging to fit our data to the expansion at this order, and we explore a strategy to systematically exclude data points and terms in the fit formulae. This strategy results in 1315 different analysis procedures. An Akaike information criterion (AIC) [54] is then employed

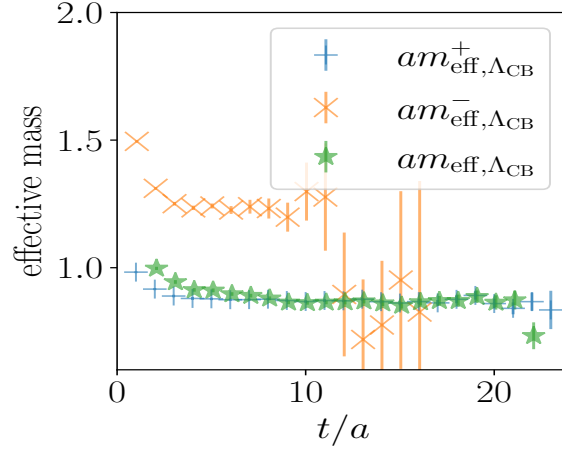


Figure 1: The Λ_{CB} baryon effective masses computed from parity-projected and unprojected correlators, on ensemble QB1 in Tab. 1 with the bare fundamental and antisymmetric valence hyperquark masses (in units of the lattice spacing, a) $am_0^{(f)} = -0.77$ and $am_0^{(as)} = -1.1$. Original plot is in Fig. 1(b) of Ref. [38].

to select the optimal procedure. Using this method, we find that for $m_{\Lambda_{\text{CB}}}$ and $m_{\Sigma_{\text{CB}}}$, the best fit function is

$$\begin{aligned} \hat{m}_{\text{CB}} = & \hat{m}_{\text{CB}}^{\chi} + F_2 \hat{m}_{\text{PS}}^2 + A_2 \hat{m}_{\text{ps}}^2 + L_1 \hat{a} \\ & + F_3 \hat{m}_{\text{PS}}^3 + A_3 \hat{m}_{\text{ps}}^3 + L_{2F} \hat{m}_{\text{PS}}^2 \hat{a} + L_{2A} \hat{m}_{\text{ps}}^2 \hat{a} \\ & + C_4 \hat{m}_{\text{PS}}^2 \hat{m}_{\text{ps}}^2, \end{aligned} \quad (14)$$

where the hatted symbols denote dimensionful quantities expressed in units of the gradient-flow scale w_0 . In the above equation, $\hat{m}_{\text{CB}}^{\chi}$, F_i , A_i , L_i and C_4 are the "low-energy constants" (LECs), to be determined by the fit. Regarding the mass of Σ_{CB}^* , the same fit function without the $C_4 \hat{m}_{\text{PS}}^2 \hat{m}_{\text{ps}}^2$ term is optimal.

Figure 2 illustrates the results of the above HBChPT-inspired analysis strategy. Plots in this figure are prepared with $L_1 = L_{2F} = L_{2A} = 0$. That is, they show the results in the continuum limit. The plot on the left-hand side exhibits results with $\hat{m}_{\text{ps}} = 0$, while that on the right-hand side is for $\hat{m}_{\text{PS}} = 0$. From these plots, it is clear that $m_{\Sigma_{\text{CB}}^*} > m_{\Lambda_{\text{CB}}} \geq m_{\Sigma_{\text{CB}}}$ in the range of the hyperquark masses that we explore. Note that this hierarchy is different from that of the analogous QCD baryons in Tab. 2. In this work, we also extrapolate the chimera baryon masses to the limit where m_{PS} and m_{ps} are both vanishing. In Fig. 3 we demonstrate these results together with the quenched meson and glueball spectra published in Refs. [30, 32].

In addition to the quenched spectrum, here we also present preliminary results of chimera baryon masses in our dynamical simulations with 2 fundamental and 3 antisymmetric Dirac flavours of hyperquarks. An effective mass plot using data from our ensemble M2 (details given in Tab. 1 of Ref. [41]) is shown in Fig. 4, where we also display results for parity-odd states. These chimera baryon masses are then exhibited together with meson masses obtained on the same ensemble in Fig. 5. Results for the excited-state mesons in this figure are extracted from an analysis using the method of generalised eigenvalue problem (GEVP) [56].

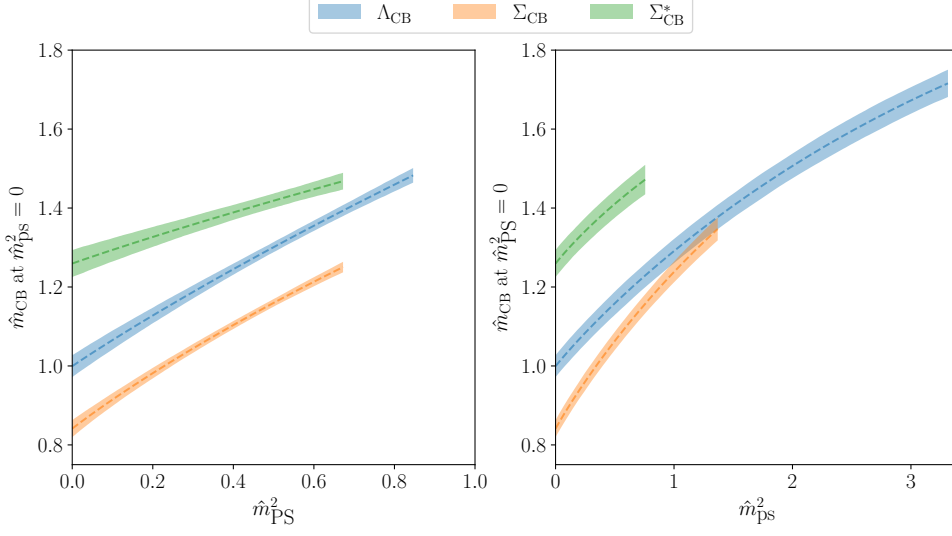


Figure 2: Mass dependence of the chimera baryons, in the continuum limit, as a function of the mass squared of the pseudoscalars, \hat{m}_{PS}^2 (left) and \hat{m}_{PS}^2 (right). Original plots are in Fig. 12 of Ref. [38].

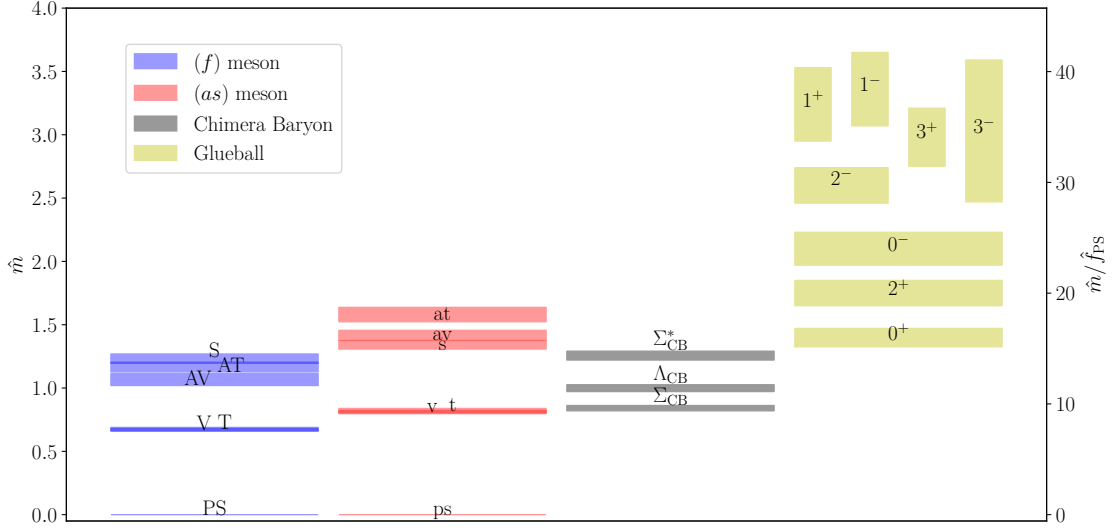


Figure 3: Meson [30], glueball [32] and chimera baryon masses in the quenched $Sp(4)$ gauge theory extrapolated to the limit of zero hyperquark masses. Glueball states are represented by the spin and parity quantum numbers with the notation J^P . In this plot, PS (ps), V (v), T(t), AV (av), AT (at) and S (s) denote the pseudoscalar, vector, tensor, axial-vector, axial-tensor and scalar mesons (off-diagonal in hyperquark flavours) made of fundamental (antisymmetric) hyperquarks. The symbol f_{PS} means the decay constant of the PS meson in the vanishing-hyperquark-mass limit. Original plot is in Fig. 13 of Ref. [38].

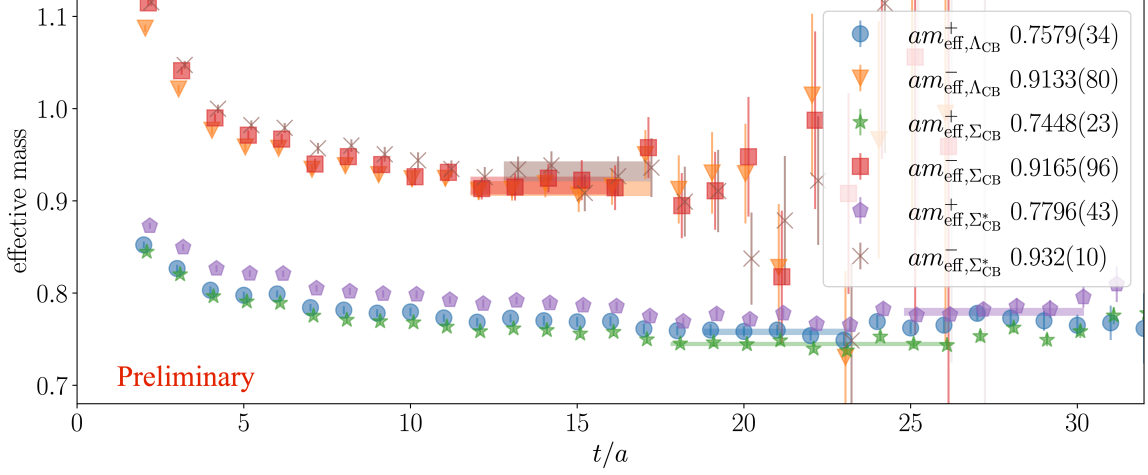


Figure 4: Ground-state chimera baryon effective masses computed on the dynamical ensemble M2 (details given in Tab. 1 of Ref. [41]). The coloured bands illustrate the fits for the masses, with the horizontal width representing the fit range, and the height indicating the statistical error. Here we display results for both parity-even and -odd states.

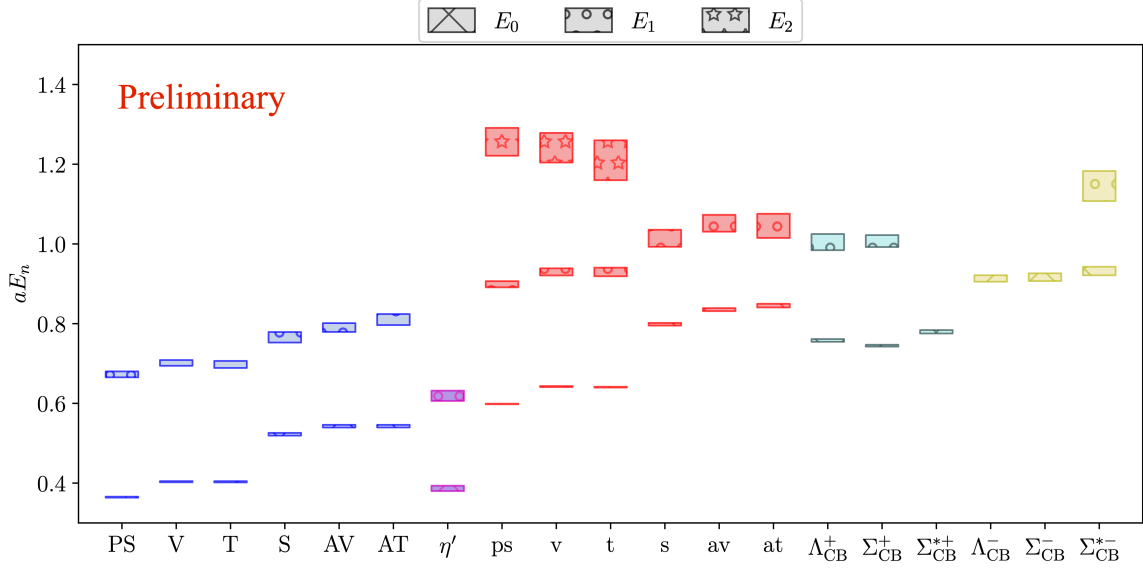


Figure 5: Masses of mesons and chimera baryons extracted from the dynamical ensemble M2 in Tab. 1 of Ref. [41]). The symbol E_0 means the ground-state mass, while E_1 and E_2 indicate the first and the second excited state masses, respectively. A GEVP method is used in the analysis. Pseudoscalar, vector, tensor, axial-vector, axial-tensor and scalar mesons (off-diagonal in hyperquark flavours) made of fundamental (antisymmetric) hyperquarks are denoted by PS (ps), V (v), T(t), AV (av), AT (at) and S (s). Description of the analysis procedure for obtaining these meson masses is reported in Ref. [55]). Furthermore, results for the flavour-singlet mesons (details in Ref. [41]), represented generically by η' , are also plotted here.

4. Conclusion and outlook

The chimera baryons in CHMs play an essential role in the implementation of the partial compositeness mechanism that facilitates the generation of the SM fermion masses, hence understanding their properties is of interest in the particle physics community. In this article, we present lattice calculations of the spectrum of low-lying chimera baryons in the $Sp(4)$ gauge theory coupled to two and three Dirac flavours of hyperquarks transforming in the fundamental and antisymmetric representations of the gauge group, respectively. Our calculation shows that candidates of the top partner, which are identified with the Λ_{CB} or Σ_{CB} , as well as the lightest spin-3/2 state, Σ_{CB}^* , are parity-even. In this article, a completed quenched computation for $m_{\Lambda_{CB}}$, $m_{\Sigma_{CB}}$ and $m_{\Sigma_{CB}^*}$ with extrapolations to the continuum limit is presented. We also discuss preliminary results of our ongoing work on calculations of these chimera baryon masses with dynamical hyperquarks.

In the future, we will also compute matrix elements entering the transitions between the top-partner candidates and the vacuum. These matrix elements are crucial input for determining the SM fermion masses from the partial compositeness mechanism, since they govern the mixing strength between SM fermions and their partner chimera baryons.

Acknowledgments

EB, BL, MP, FZ acknowledge the STFC DTP Grant No. ST/X000648/1. EB and BL are grateful for the support of their work from the EPSRC ExCALIBUR programme ExaTEPP (project EP/ X017168/1). EB also acknowledges the STFC Research Software Engineering Fellowship EP/V052489/1. The work of NF is supported by the STFC Doctoral Training Grant No. ST/X508834/1. DKH acknowledges support from Basic Science Research Program through the National Research Foundation of Korea (NRF) funded by the Ministry of Education (NRF-2017R1D1A1B06033701), as well as the NRF grant MSIT 2021R1A4A5031460 from the Korean government. JWL acknowledges support from Institute for Basic Science through the project code IBS-R018-D1. HH and CJDL acknowledges support from NSTC Taiwan, through grant number 112-2112-M-A49-021-MY3. CJDL also receives support from two other NSTC grants, 112-2639-M-002-006-ASP and 113-2119-M-007-013. DV acknowledges support from STFC through Consolidated Grant No. ST/X000680/1. BL and MP are also funded by STFC through Consolidated Grant No. ST/T000813/1, as well as by the European Research Council (ERC) through Horizon 2020 research and innovation program of the European Union, through Grant Agreement No. 813942.

This work used the DiRAC Data Intensive service CSD3 at the University of Cambridge, managed by the University of Cambridge University Information Services; the DiRAC Data Intensive service DiAL at the University of Leicester, managed by the University of Leicester Research Computing Service; and the DiRAC Extreme Scaling service Tursa at the University of Edinburgh, managed by the Edinburgh Parallel Computing Centre; all on behalf of the STFC DiRAC HPC Facility (www.dirac.ac.uk), and each of which was funded by BEIS, UKRI and STFC capital funding and STFC operations grants. DiRAC is part of the UKRI Digital Research Infrastructure. We acknowledge the support of the Supercomputing Wales programme, which was part-funded by the European Regional Development Fund via Welsh Government.

Open Access Statement—For the purpose of open access, the authors have applied a Creative Commons Attribution (CC BY) licence to any Author Accepted Manuscript version arising.

Research Data Access Statement—The results reported here are based on preliminary analysis. Further analysis and the data generated for this manuscript will be released together with an upcoming publication. Alternatively, preliminary data and code can be obtained from the authors upon request.

References

- [1] M. Aizenman and H. Duminil-Copin, *Annals Math.* **194**, 163 (2021), [1912.07973](#).
- [2] M. Luscher and P. Weisz, *Nucl. Phys. B* **290**, 25 (1987).
- [3] M. Luscher and P. Weisz, *Nucl. Phys. B* **295**, 65 (1988).
- [4] M. Luscher and P. Weisz, *Nucl. Phys. B* **318**, 705 (1989).
- [5] J. Bulava, P. Gerhold, K. Jansen, J. Kallarackal, B. Knippschild, C. J. D. Lin, K.-I. Nagai, A. Nagy, and K. Ogawa, *Adv. High Energy Phys.* **2013**, 875612 (2013), [1210.1798](#).
- [6] E. Mølgaard and R. Shrock, *Phys. Rev. D* **89**, 105007 (2014), [1403.3058](#).
- [7] D. Y. J. Chu, K. Jansen, B. Knippschild, and C. J. D. Lin, *JHEP* **01**, 110 (2019), [1811.05667](#).
- [8] K. Kajantie, M. Laine, K. Rummukainen, and M. E. Shaposhnikov, *Phys. Rev. Lett.* **77**, 2887 (1996), [hep-ph/9605288](#).
- [9] M. Laine, G. Nardini, and K. Rummukainen, *JCAP* **01**, 011 (2013), [1211.7344](#).
- [10] G. Panico and A. Wulzer, **913** (2016), [1506.01961](#).
- [11] G. Cacciapaglia, C. Pica, and F. Sannino, *Phys. Rept.* **877**, 1 (2020), [2002.04914](#).
- [12] G. Cacciapaglia, G. Ferretti, T. Flacke, and H. Serôdio, *Front. in Phys.* **7**, 22 (2019), [1902.06890](#).
- [13] J. Barnard, T. Gherghetta, and T. S. Ray, *JHEP* **02**, 002 (2014), [1311.6562](#).
- [14] G. Ferretti and D. Karateev, *JHEP* **03**, 077 (2014), [1312.5330](#).
- [15] M. E. Peskin, *Nucl. Phys. B* **175**, 197 (1980).
- [16] D. B. Kaplan, *Nucl. Phys. B* **365**, 259 (1991).
- [17] R. Arthur, V. Drach, M. Hansen, A. Hietanen, C. Pica, and F. Sannino, *Phys. Rev. D* **94**, 094507 (2016), [1602.06559](#).
- [18] V. Drach, T. Janowski, C. Pica, and S. Prelovsek, *JHEP* **04**, 117 (2021), [2012.09761](#).
- [19] V. Drach, P. Fritzscht, A. Rago, and F. Romero-López, *Eur. Phys. J. C* **82**, 47 (2022), [2107.09974](#).

- [20] T. DeGrand, Y. Liu, E. T. Neil, Y. Shamir, and B. Svetitsky, *Phys. Rev. D* **91**, 114502 (2015), [1501.05665](#).
- [21] T. A. DeGrand, M. Golterman, W. I. Jay, E. T. Neil, Y. Shamir, and B. Svetitsky, *Phys. Rev. D* **94**, 054501 (2016), [1606.02695](#).
- [22] V. Ayyar, T. DeGrand, M. Golterman, D. C. Hackett, W. I. Jay, E. T. Neil, Y. Shamir, and B. Svetitsky, *Phys. Rev. D* **97**, 074505 (2018), [1710.00806](#).
- [23] V. Ayyar, T. DeGrand, D. C. Hackett, W. I. Jay, E. T. Neil, Y. Shamir, and B. Svetitsky, *Phys. Rev. D* **97**, 114505 (2018), [1801.05809](#).
- [24] V. Ayyar, T. DeGrand, D. C. Hackett, W. I. Jay, E. T. Neil, Y. Shamir, and B. Svetitsky, *Phys. Rev. D* **97**, 114502 (2018), [1802.09644](#).
- [25] V. Ayyar, T. DeGrand, D. C. Hackett, W. I. Jay, E. T. Neil, Y. Shamir, and B. Svetitsky, *Phys. Rev. D* **99**, 094502 (2019), [1812.02727](#).
- [26] G. Cossu, L. Del Debbio, M. Panero, and D. Preti, *Eur. Phys. J. C* **79**, 638 (2019), [1904.08885](#).
- [27] L. Del Debbio, A. Lupo, M. Panero, and N. Tantalo, *Eur. Phys. J. C* **83**, 220 (2023), [2211.09581](#).
- [28] E. Bennett, D. K. Hong, J.-W. Lee, C. J. D. Lin, B. Lucini, M. Piai, and D. VDACCHINO, *JHEP* **03**, 185 (2018), [1712.04220](#).
- [29] E. Bennett, D. K. Hong, J.-W. Lee, C. J. D. Lin, B. Lucini, M. Piai, and D. VDACCHINO, *JHEP* **12**, 053 (2019), [1909.12662](#).
- [30] E. Bennett, D. K. Hong, J.-W. Lee, C.-J. D. Lin, B. Lucini, M. Mesiti, M. Piai, J. Rantaharju, and D. VDACCHINO, *Phys. Rev. D* **101**, 074516 (2020), [1912.06505](#).
- [31] E. Bennett, J. Holligan, D. K. Hong, J.-W. Lee, C. J. D. Lin, B. Lucini, M. Piai, and D. VDACCHINO, *Phys. Rev. D* **102**, 011501 (2020), [2004.11063](#).
- [32] E. Bennett, J. Holligan, D. K. Hong, J.-W. Lee, C. J. D. Lin, B. Lucini, M. Piai, and D. VDACCHINO, *Phys. Rev. D* **103**, 054509 (2021), [2010.15781](#).
- [33] E. Bennett, D. K. Hong, H. Hsiao, J.-W. Lee, C. J. D. Lin, B. Lucini, M. Mesiti, M. Piai, and D. VDACCHINO, *Phys. Rev. D* **106**, 014501 (2022), [2202.05516](#).
- [34] E. Bennett, D. K. Hong, J.-W. Lee, C. J. D. Lin, B. Lucini, M. Piai, and D. VDACCHINO, *Phys. Lett. B* **835**, 137504 (2022), [2205.09254](#).
- [35] E. Bennett, D. K. Hong, J.-W. Lee, C. J. D. Lin, B. Lucini, M. Piai, and D. VDACCHINO, *Phys. Rev. D* **106**, 094503 (2022), [2205.09364](#).
- [36] E. Bennett, J. Holligan, D. K. Hong, H. Hsiao, J.-W. Lee, C. J. D. Lin, B. Lucini, M. Mesiti, M. Piai, and D. VDACCHINO, *Universe* **9**, 236 (2023), [2304.01070](#).

- [37] E. Bennett et al., Phys. Rev. D **108**, 094508 (2023), [2306.11649](#).
- [38] E. Bennett, D. K. Hong, H. Hsiao, J.-W. Lee, C. J. D. Lin, B. Lucini, M. Piai, and D. VDACCHINO, Phys. Rev. D **109**, 094512 (2024), [2311.14663](#).
- [39] E. Bennett, J. Holligan, D. K. Hong, J.-W. Lee, C. J. D. Lin, B. Lucini, M. Piai, and D. VDACCHINO, Phys. Rev. D **109**, 094517 (2024), [2312.08465](#).
- [40] E. Bennett et al., Phys. Rev. D **110**, 074509 (2024), [2405.01388](#).
- [41] E. Bennett, N. Forzano, D. K. Hong, H. Hsiao, J.-W. Lee, C. J. D. Lin, B. Lucini, M. Piai, D. VDACCHINO, and F. ZIERLER, Phys. Rev. D **110**, 074504 (2024), [2405.05765](#).
- [42] E. Bennett, D. K. Hong, H. Hsiao, J.-W. Lee, C. J. D. Lin, B. Lucini, M. Piai, and D. VDACCHINO (2024), [2412.01170](#).
- [43] S. Kulkarni, A. Maas, S. Mee, M. Nikolic, J. Pradler, and F. Zierler, SciPost Phys. **14**, 044 (2023), [2202.05191](#).
- [44] E. Bennett, H. Hsiao, J.-W. Lee, B. Lucini, A. Maas, M. Piai, and F. Zierler, Phys. Rev. D **109**, 034504 (2024), [2304.07191](#).
- [45] Y. Dengler, A. Maas, and F. Zierler, Phys. Rev. D **110**, 054513 (2024), [2405.06506](#).
- [46] E. Bennett, B. Lucini, D. Mason, M. Piai, E. Rinaldi, and D. VDACCHINO (2024), [2409.19426](#).
- [47] E. Bennett, D. K. Hong, H. Hsiao, J.-W. Lee, C. J. D. Lin, B. Lucini, M. Piai, and D. VDACCHINO, *Lattice investigations of the chimera baryon spectrum in the $Sp(4)$ gauge theory—Data release, 10.5281/zenodo.10819721* (2024).
- [48] E. Bennett, D. K. Hong, H. Hsiao, J.-W. Lee, C. J. D. Lin, B. Lucini, M. Piai, and D. VDACCHINO, in preparation.
- [49] S. Borsányi, S. Dürr, Z. Fodor, C. Hoelbling, S. D. Katz, S. Krieg, T. Kurth, L. Lellouch, T. Lippert, and C. McNeile (BMW), JHEP **09**, 010 (2012), [1203.4469](#).
- [50] A. Banerjee, D. B. Franzosi, and G. Ferretti, JHEP **03**, 200 (2022), [2202.00037](#).
- [51] E. E. Jenkins and A. V. Manohar, Phys. Lett. B **255**, 558 (1991).
- [52] V. Bernard, N. Kaiser, and U.-G. Meissner, Int. J. Mod. Phys. E **4**, 193 (1995), [hep-ph/9501384](#).
- [53] S. R. Beane and M. J. Savage, Phys. Rev. D **68**, 114502 (2003), [hep-lat/0306036](#).
- [54] H. Akaike, Springer Science+Business Media (1998).
- [55] H. Hsiao, E. Bennett, N. Forzano, D. K. Hong, J.-W. Lee, C. J. D. Lin, B. Lucini, M. Piai, D. VDACCHINO, and F. Zierler, PoS LATTICE2024, 139 (2025), [2411.18379](#).
- [56] M. Luscher and U. Wolff, Nucl. Phys. B **339**, 222 (1990).